Supplementary information for:

Tuning the water reduction through controlled nanoconfinement within an organic liquid matrix

Nicolas Dubouis[1,2,5], Alessandra Serva[3,5], Roxanne Berthin[3,5], Guillaume Jeanmairet[3,5], Benjamin Porcheron[4,5], Elodie Salager[4,5], Mathieu Salanne[3,5,*], Alexis Grimaud[1,2,5,*]

1. Chimie du Solide et de l'Energie, Collège de France, UMR 8260, 75231 Paris Cedex 05

2. Sorbonne Université, Paris, France

3. Sorbonne Université, CNRS, Physico-Chimie des Électrolytes et Nanosystèmes Interfaciaux, F-75005 Paris, France

4. CNRS-CEMHTI, UPR3079, Université d'Orléans, 1D avenue de la recherche scientifique, 45071 Orléans Cedex, France

5. Réseau sur le Stockage Electrochimique de l'Energie (RS2E), CNRS FR3459, 33 rue Saint Leu, 80039 Amiens Cedex, France

***Corresponding authors :**

Alexis Grimaud : alexis.grimaud@college-de-france.fr

Mathieu Salanne : mathieu.salanne@sorbonne-universite.fr

Physico-chemical properties of the different electrolytes studied and details of the simulations for the bulk electrolytes

Supplementary Table 1. Physical properties for the electrolytes containing 100 mM $LiClO_4$ and different water contents, as well as details for the simulation box (Figure 4 in the main text).

Water content (weight%)	1%	2.5%	5%	7.5%	10%
Density ($g.cm^{-3}$)	0.773	0.773	0.775	0.789	0.784
[H_2O] ($mol.L^{-1}$)	0.420	1.03	2.02	3.01	3.96
[$LiClO_4$] ($mol.L^{-1}$)	0.096	0.095	0.092	0.092	0.091
Box Length (Å)	44.08		44.70		45.02
Number ACN	965		966		966
Number H_2O	22		110		220
Number $LiClO_4$	5		5		5

Supplementary Table 2. Physical properties for the electrolytes containing 100 mM $TBAClO_4$ and different water contents, as well as details for the simulation box (Figure 3 in the main text).

Water content (weight%)	1%	2.5%	5%	7.5%	10%
Density ($g.cm^{-3}$)	0.769	0.775	0.781	0.783	0.792
[H_2O] ($mol.L^{-1}$)	0.422	1.05	2.06	3.03	3.99
[$TBAClO_4$] ($mol.L^{-1}$)	0.097	0.096	0.094	0.092	0.091
Box Length (Å)	44.94		44.59		45.07
Number ACN	965		966		966
Number H_2O	22		110		220
Number $TBAClO_4$	5		5		5

Supplementary Table 3. Physical properties for the electrolytes containing 10% in mass of H_2O at different Li/H_2O molar ratio and simulation box details (Figure 5 in the main text).

Li/H_2O molar ratio	0.02	0.11	0.22	0.45
Density ($g.cm^{-3}$)	0.784	0.819	0.853	0.914
[H_2O] ($mol.L^{-1}$)	3.96	3.89	3.83	3.70
[$LiClO_4$] ($mol.L^{-1}$)	0.091	0.445	0.878	1.69
Box Length (Å)	45.02	45.45	45.68	
Number ACN	966	966	966	
Number H_2O	220	220	220	
Number $LiClO_4$	5	25	50	

Molecular Dynamics Simulations at constant applied voltage

Supplementary Table 4. Simulation box details for $LiClO_4$-based electrolytes between two planar graphite electrodes.

Number $LiClO_4$	Number ACN	Number H_2O	Box Volume (Å^3)	Density (g.cm^{-3})
20	3860	88	34.10 x 36.89 x 290.69	0.786
20	3864	880	34.10 x 36.89 x 312.13	0.794
100	1932	440	34.10 x 36.89 x 173.15	0.853

The electrolyte is put in between two planar graphite electrodes, each of them consisting in three layers of graphene (1440 carbon atoms per electrode).

Calculation of the X-ray-weighted structure factors

The X-Ray weighted structure factors were determined using:

$$S(q) = 1 + \frac{\sum_i \sum_j c_i c_j w_i(k) w_j^*(k) \left[S_{ij}(k) - 1\right]}{\left|\sum_i c_i w_i(k)\right|^2} \quad \text{(Eq. S1)}$$

where q is the scattering vector magnitude, c_i the atomic fraction of the atom i and $w_i$is the atomic form factor obtained from ref. 1[1], and S_{ij} the partial structure factor that is obtained by a Fourier transform of the partial distribution function:

$$S_{ij}(q) = 1 + \frac{4\pi\rho}{q} \int_0^\infty r\left[g_{ij}(r) - 1\right] \sin(qr)\, dr \quad \text{(Eq. S2)}$$

where ρ is the atomic number density of the electrolyte (number of atomes in the box divided by the box volume) and $g_{ij}(r)$ the partial distribution function.

Supplementary Figures

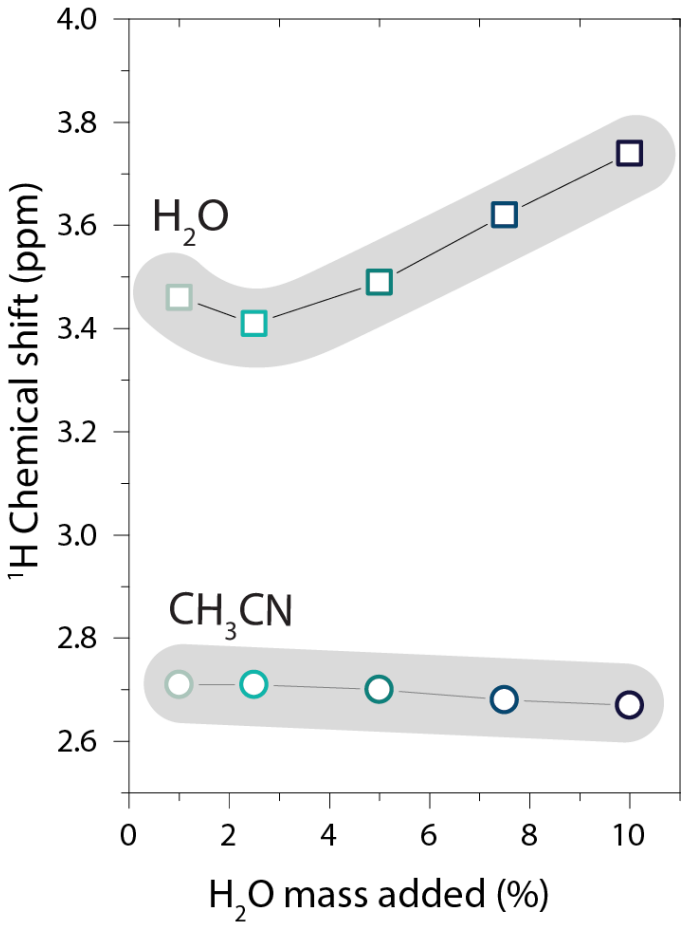

Supplementary Figure 1. ^{1}H chemical shift for H_2O (squares) and acetonitrile CH_3CN (ACN, circles) molecules for different water contents in acetonitrile with 100 mM $LiClO_4$. The almost steady chemical shift of the **–CH_3** group of acetonitrile as a function of the water concentration confirms that the trend measured for the ^{1}H chemical shifts of protons from H_2O is not related to a change in the electrolytes magnetic susceptibility. The lines are guide for the eyes.

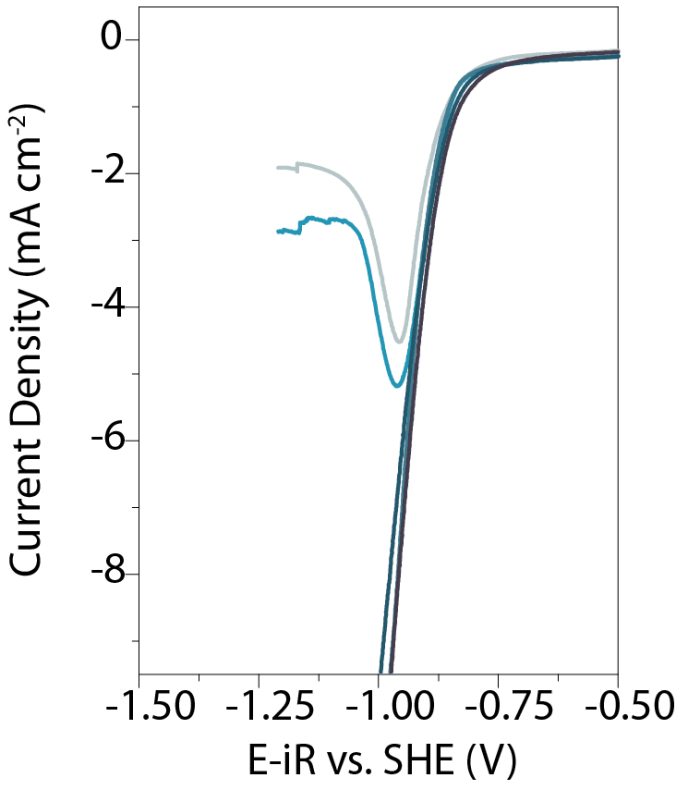

Supplementary Figure 2. Linear sweep voltammograms recorded in acetonitrile in presence of 100 mM LiTFSI with different water contents (1, 2.5, 5, 7.5 and 10% from light to dark blue) using a rotating disk (1 600 rpm) Pt electrode with a 50 mV s^{-1} sweeping rate. No modification of the onset potential at which water is reduced was observed, independently of the water content, confirming that the trend previously measured for $LiClO_4$ is independent on the nature of the anion.

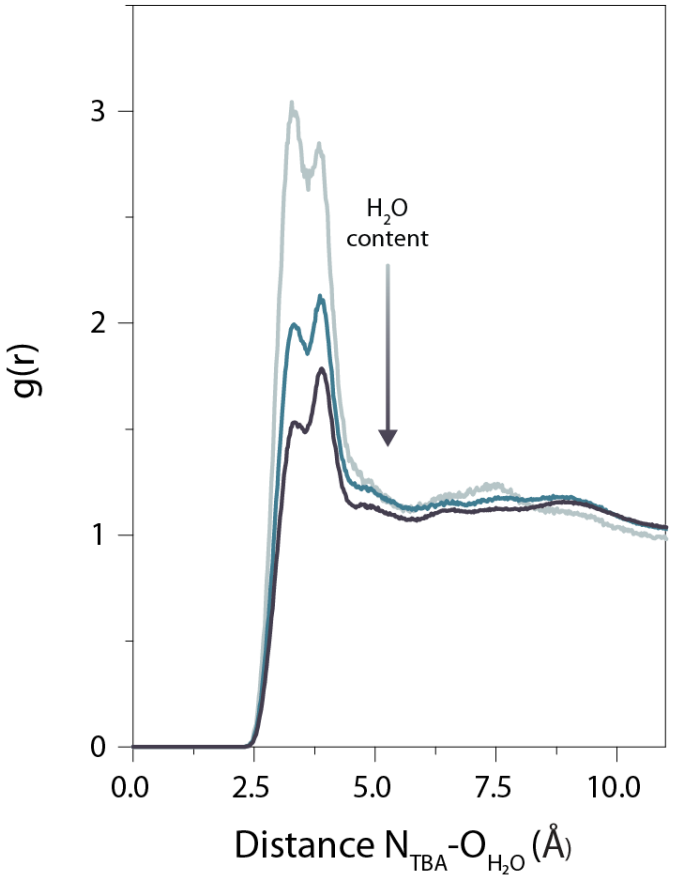

Supplementary Figure 3. TBA-O(H_2O) radial distribution functions, g(r)'s, computed from the MD simulations for electrolytes containing 100 mM $TBAClO_4$ at different water contents (1% in light blue, 5% in blue and 10% in dark blue) in acetonitrile. The broadness of the first peak in the g(r) reflects the hydrophobic character of TBA^+ cations.

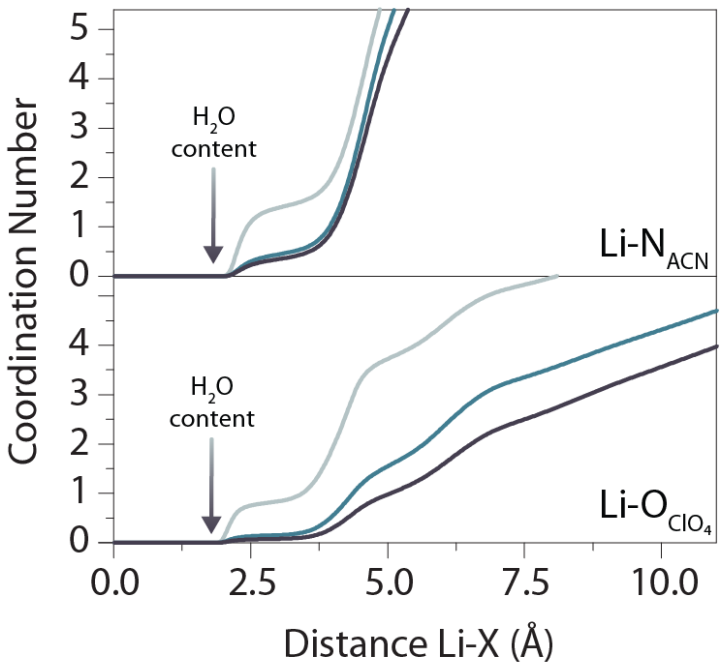

Supplementary Figure 4. Coordination number between Li^+ cations and nitrogen atoms from acetonitrile molecules (top) and oxygen atoms from ClO_4^- anions (bottom) in the presence of electrolytes containing 100 mM $LiClO_4$ at different water content (1% in light blue, 5% in blue and 10% in dark blue) in acetonitrile. The decrease of the first plateau intensity with the water content shows that water molecules replace acetonitrile and perchlorate anions in the Li^+ cation first solvation shell when the concentration of water is increased in the electrolytes.

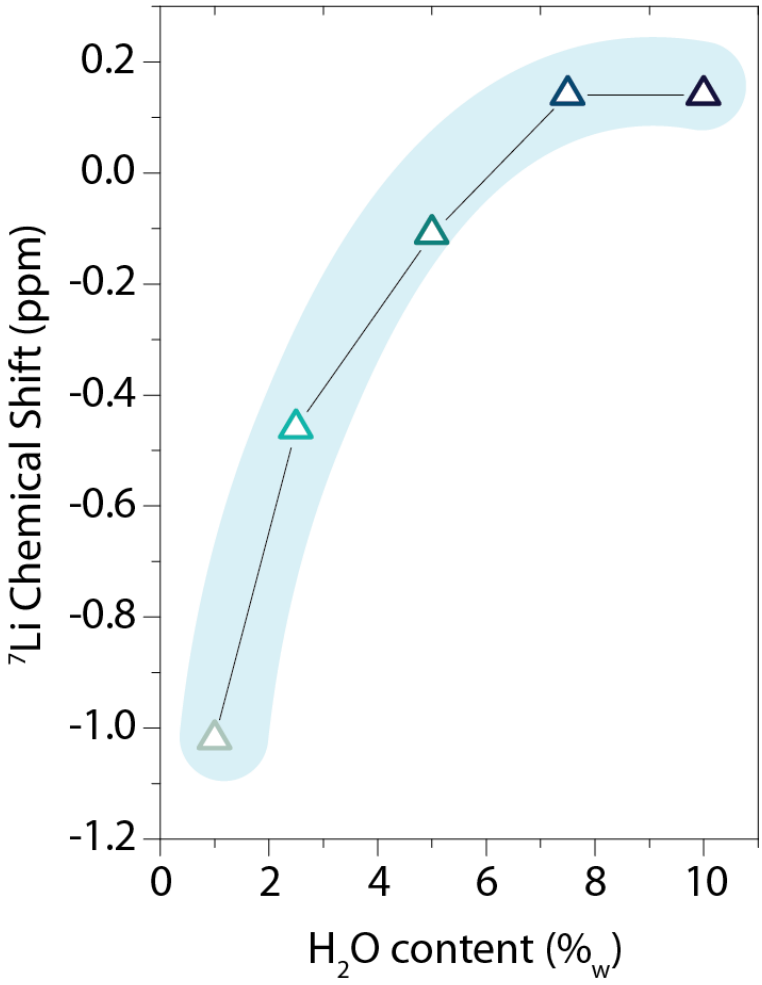

Supplementary Figure 5. Evolution of the ^{7}Li chemical shift in the presence of 100 mM $LiClO_4$ in acetonitrile as a function of the water content. The chemical shifts measured at high water contents (> 7.5%) slightly above 0 ppm are close to values measured in aqueous electrolytes (0 ppm is defined by the ^{7}Li resonance frequency in a 1M LiCl aqueous solution). The negative values measured at lower water-content may result from a shielding from the ACN or ClO_4^- anions.[2] The line is a guide for the eye.

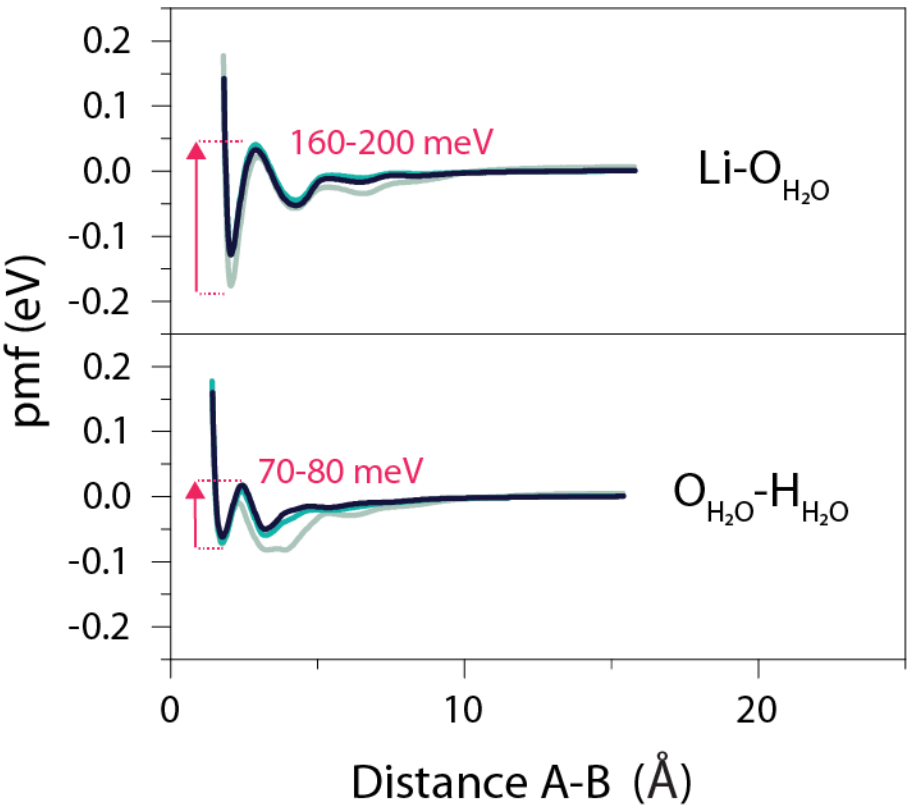

Supplementary Figure 6. Potential of mean force between Li^+ cations and O_{water} (top) and between O_{water} and H_{water} (bottom) derived from the g(r) functions. $pmf(r) = -k_B T \ln g(r)$, where k_B is the Boltzmann constant and T the temperature (300K) for different water contents (1% in light blue, 5% in blue and 10% in dark blue). Since the largest values are obtained for Li-O_{water}, independently on the water content, this indicates that it is more difficult to separate one Li^+ cation from a water molecule than a water molecule from another one.

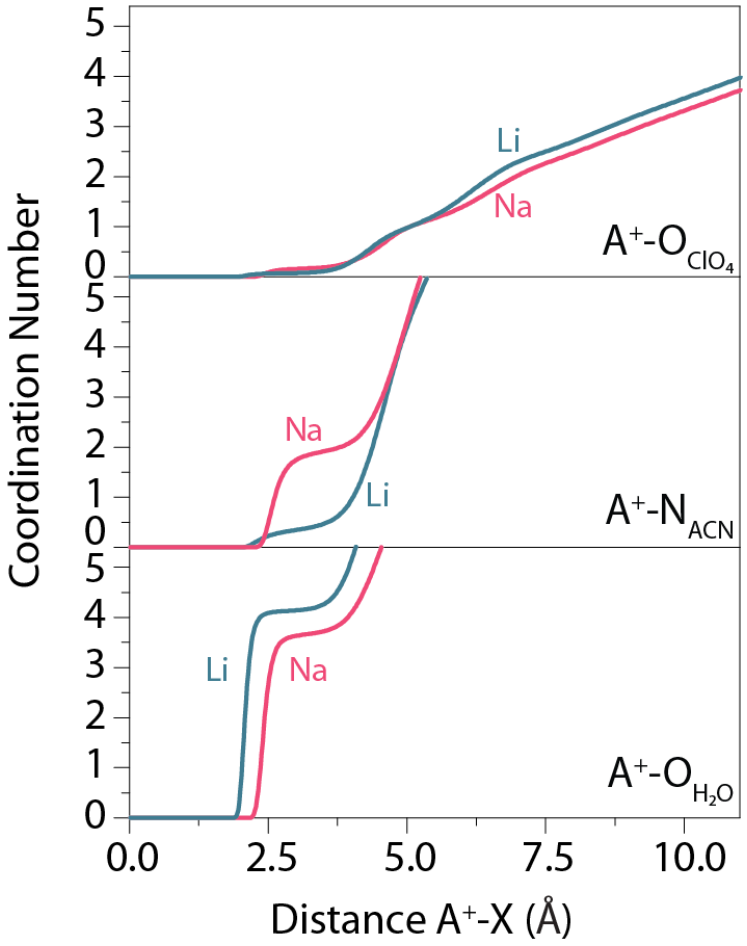

Supplementary Figure 7. Coordination number between Li^+ cation (blue) or Na^+ cations (pink) and oxygen atoms from ClO_4^- anions (top), nitrogen atoms from acetonitrile molecules (middle) and oxygen atoms from water molecules (bottom) in the presence of 100 mM of $ACIO_4$ in acetonitrile containing 10% of water in mass. The simulation box for $NaClO_4$ was similar to the $LiClO_4$ one (Supplementary Table 1) and the Lennard-Jones parameters for Na^+ were chosen from Åqvist.[3] The number of water molecules and ClO_4^- anions present in the first solvation shell of the Na^+ and Li^+ cations is similar, while more acetonitrile is found in the case of Na^+.

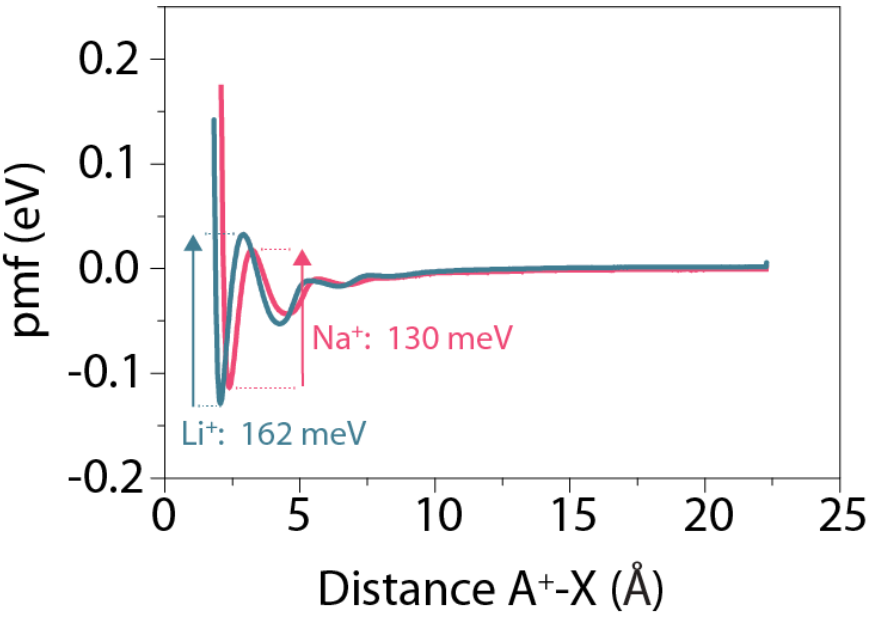

Supplementary Figure 8. Potential of mean force between Li^+ or Na^+ cations and O_{water} (derived from the g(r) functions ($pmf(r) = -k_B T \ln g(r)$, where k_B is the Boltzmann constant and T the temperature (300K)) in acetonitrile containing 10% of water in mass and 100 mM of $LiClO_4$ or $NaClO_4$ salt. Since a smaller value is predicted in the presence of Na^+ cations, this indicates that the water-Na^+ interaction is weaker when compared to the water-Li^+ interaction.

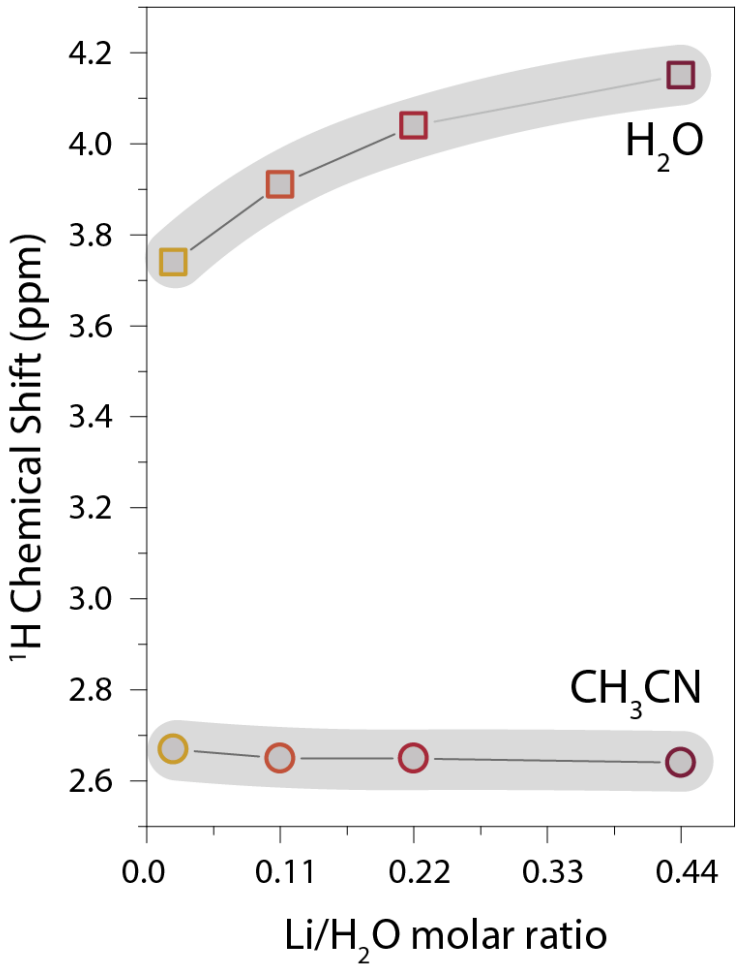

Supplementary Figure 9. ^{1}H chemical shift H_2O (squares) and acetonitrile CH_3CN (ACN, circles) molecules for different lithium content in acetonitrile containing 10% of water in mass. The very weak modification of the chemical shift of the acetonitrile **–CH_3** group with the lithium concentration confirms that the trends measure for H_2O protons are not related to a change in the magnetic susceptibility of the electrolytes. The corresponding H_2O/Li ratios are: 44 (yellow), 8.8 (orange), 4.4 (red) and 2.2 (brown). The lines are guides for the eyes.

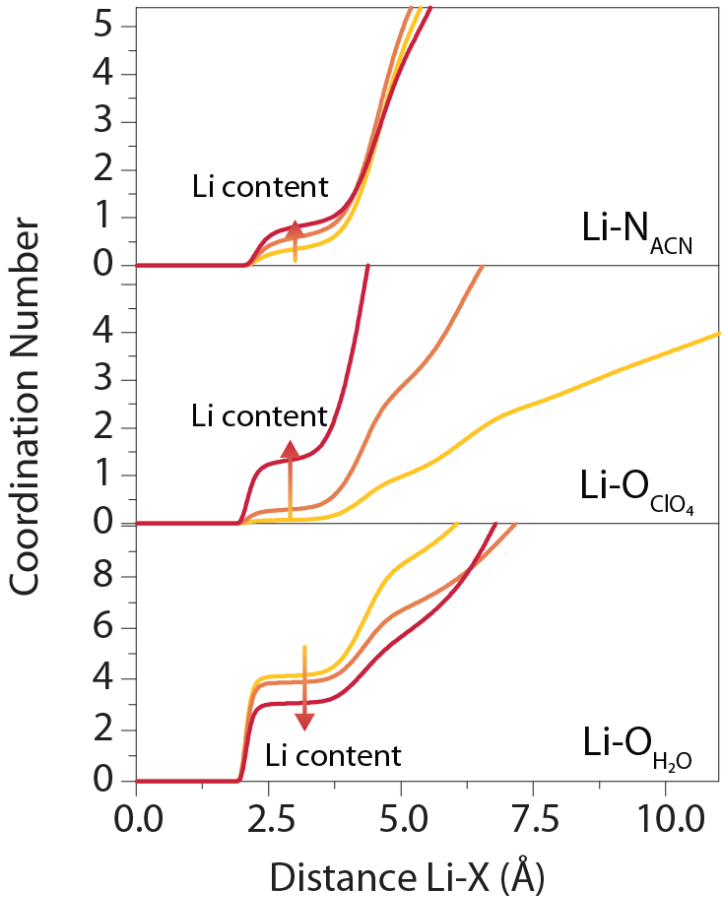

Supplementary Figure 10. Coordination number between Li^+ cations and nitrogen atoms from acetonitrile molecules (top) and oxygen atoms from ClO_4^- anions (middle) and oxygen atoms from water molecules (bottom) in acetonitrile containing 10% of water in mass at different H_2O/Li ratio (44 yellow, 8.8 orange, 4.4 red). The increase of the $LiClO_4$ concentration results in an increased amplitude of the first plateau of the Li-O(ClO_4^-) coordination number, which suggests more ion-pairing, accompanied by a small increase of the acetonitrile in the first solvation shell of Li^+ cations and a small decrease of the water content in the first solvation shell.

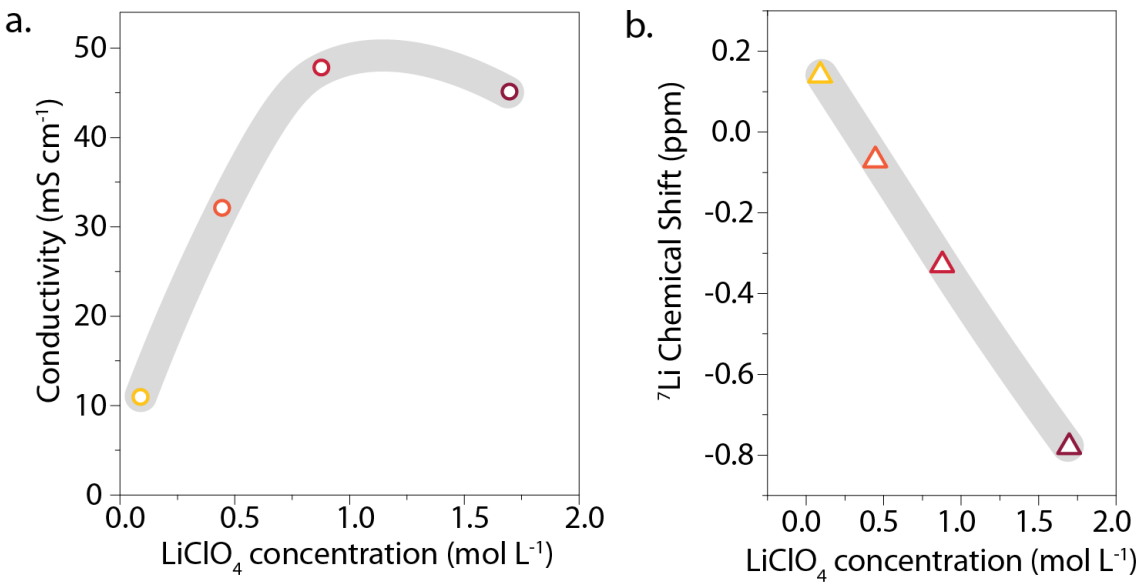

Supplementary Figure 11. a. Evolution of the electrolyte (acetonitrile with 10% of water in mass) conductivity and **b.** ^{7}Li chemical shift with the $LiClO_4$ concentration. The indicated concentrations correspond to the electrolytes previously studied with different Li/H_2O ratios (Supplementary Table 3). The bell shape for the conductivity and the downfield of the ^{7}Li suggest that ion-pairs are formed when the salt concentration is increased. The lines are guides for the eyes.

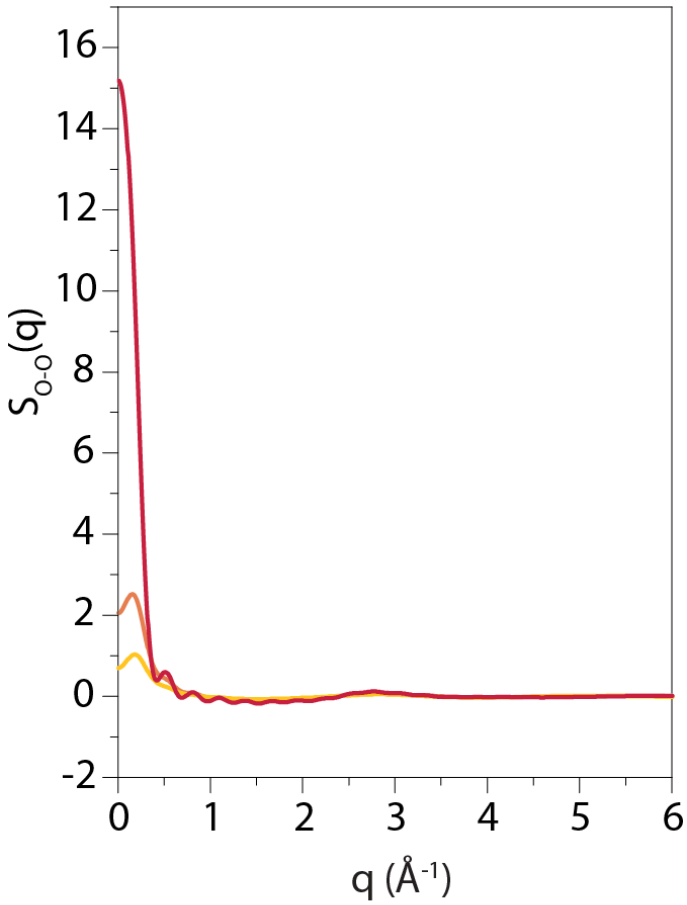

Supplementary Figure 12. X-Ray weighted contributions from the oxygen-oxygen pairs to the global X-ray-weighted structure factor obtained from the MD simulations for acetonitrile electrolytes containing 10% of water in mass at different H_2O/Li ratio (44 yellow, 8.8 orange, 4.4 red).

Supplementary Table 5. Activation energies measured by PFG NMR. Uncertainties were evaluated by fitting the data for all possible permutations of 4 temperatures out of 5

Sample	10% H_2O 1M $LiClO_4$	10% H_2O 100 mM $LiClO_4$
E_a(**H**$_2$O) (kJ.mol^{-1})	28±3	31±5
E_a(C**H$_3$**CN) (kJ.mol^{-1})	23±3	30±7
E_a(Li, fast) (kJ.mol^{-1})	32±6	42±4
E_a (Li, slow) (kJ.mol^{-1})	92.2	

The data were processed and integrated in the Bruker Topspin software. The water and acetonitrile ^{1}H peaks are well resolved and were fitted independently. The self-diffusion coefficients were obtained in Matlab (The Mathworks, Inc.), using a weighted least-square-fit (polyfitweighted, 2006, S.S. Rogers) to the equation $\ln(A) = \alpha - BD$, with A the area of the signal, D the self-diffusion coefficient and $B = (\Delta - \frac{\delta}{3})(2\pi\gamma G\delta)^2$, Δ the effective diffusion time, δ the effective gradient duration, γ the gyromagnetic ratio and G the PFG strength. For the (ACN 10% of H_2O, 1M LiClO4) sample at 310 K and 318 K, the ^{7}Li data required 2 components and a non-linear fit to $A = \propto_1 \exp(-B_1D_1) + \propto_2 \exp(-B_2D_2)$ was performed using the nlinfit Matlab funtion. The uncertainties are given as ±2 standard deviations in the figures. The activation energies were then obtained using a least-square fit (Arrhenius law) in Matlab. Diffusion coefficients and corresponding fits are given in the Supplementary Figure 13.

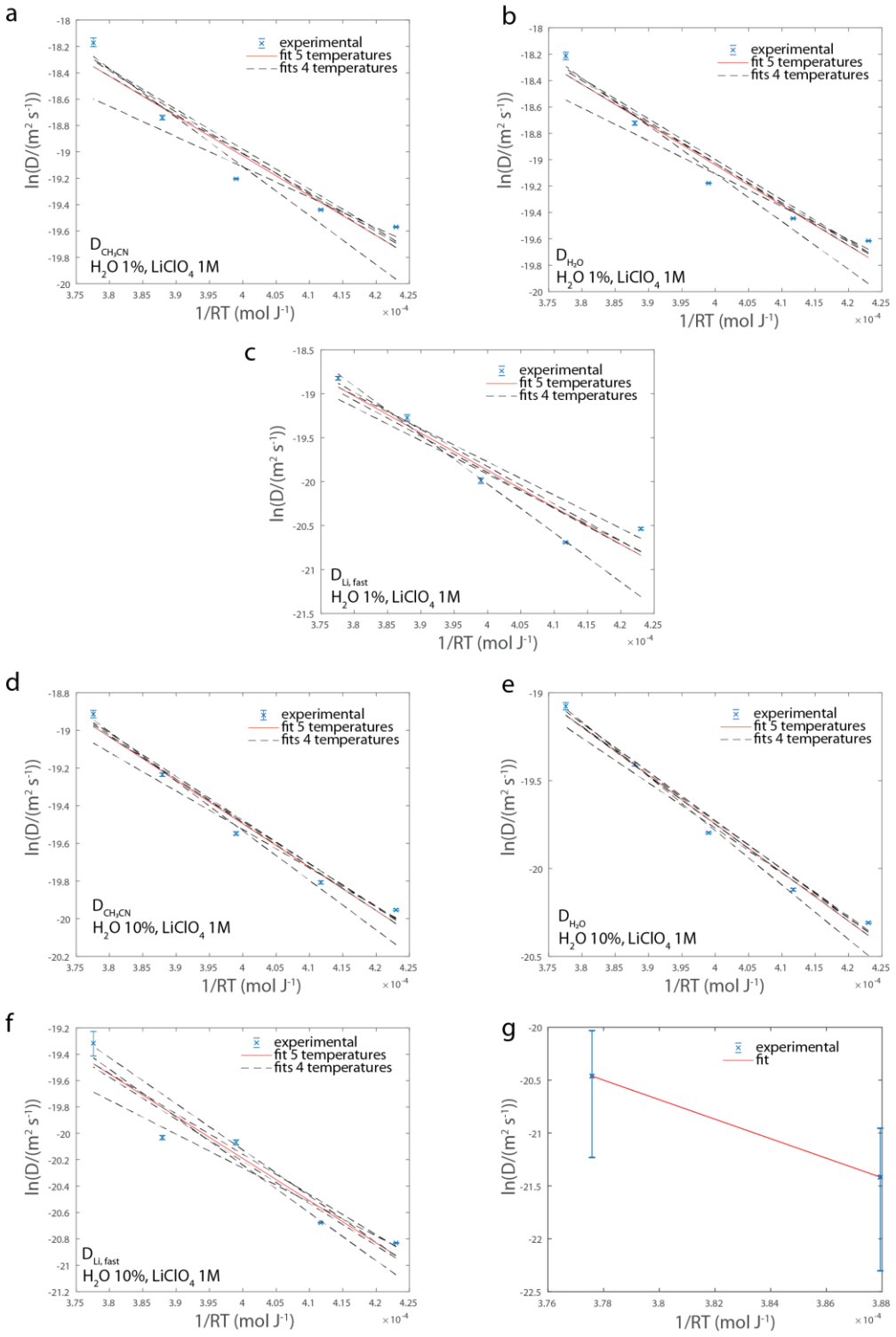

Supplementary Figure 13. Arrhenius fits for the self-diffusion coefficients in the 10% H_2O 100 mM $LiClO_4$ electrolyte for a) CH_3CN, b) H_2O, c) Li^+ and in the 10% H_2O 1M $LiClO_4$ electrolyte for d) CH_3CN, e) H_2O, f) Li^+ (fast) and g) Li^+ (fast).

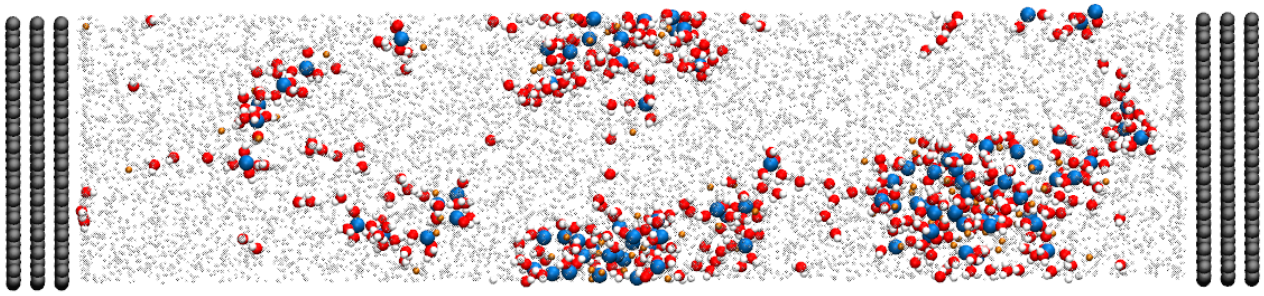

Supplementary Figure 14. Snapshot extracted from the MD simulation at constant applied potential of 1 V for the system rich in water and lithium (acetonitrile that contains 10% of water in mass with a H_2O/Li ratio = 4.4, see Supplementary Table 3). The positive carbon electrode is on the left while the negative one is on the right.

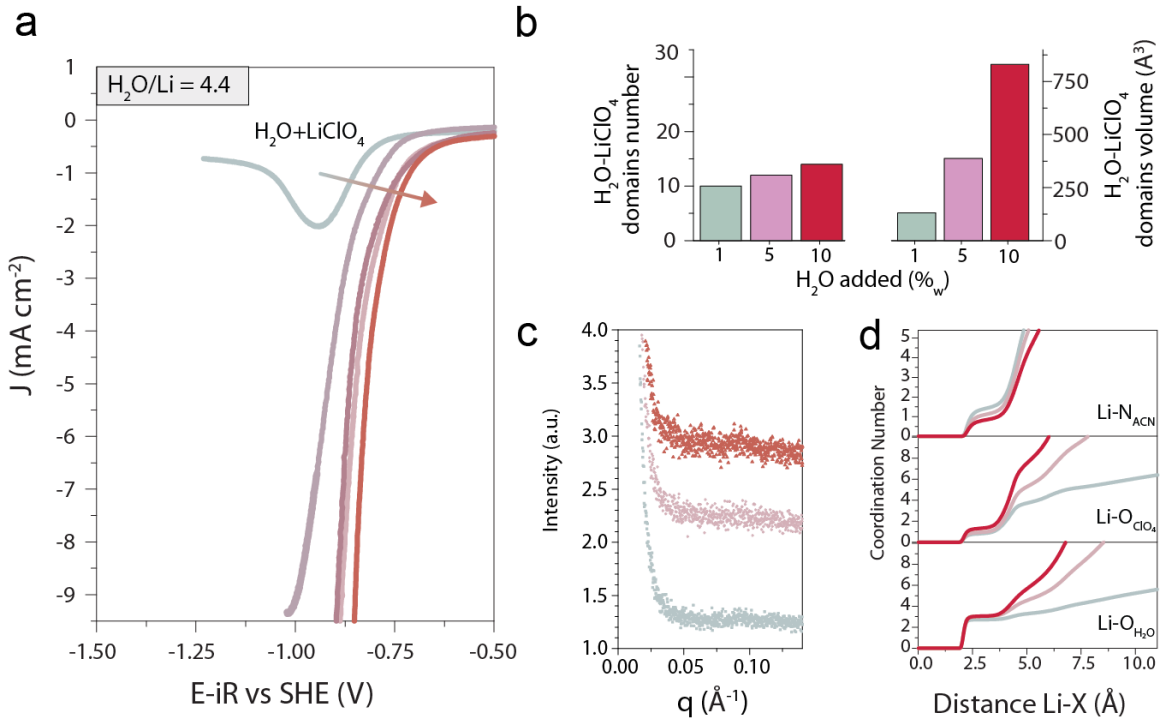

Supplementary Figure 15. a) Linear sweep voltammograms recorded in acetonitrile with a H_2O/Li^+ ratio of 4.4 at different water concentration (from 1% light grey, to 10% red) on a rotating disk (1 600 rpm) Pt electrode with a 50 mV s^{-1} sweeping rate. **b)** Number of $LiClO_4$-H_2O domains and their average volume depending on the $LiClO_4/H_2O$ ratio at 10% of water concentration extracted from the MD simulations. **c)** SAXS intensity in the low-q range of acetonitrile for the electrolytes with 1% (grey), 5% (rose) or 10% of added H_2O at constant H_2O/Li^+ ration of 4.4 and **d)** corresponding coordination numbers between the Li^+ cations and acetonitrile molecules (top), ClO_4^- anions (middle) and water molecules (bottom). The simulation box for the 5% H_2O electrolyte contains 966 acetonitrile molecules, 110 water molecules and 25 $LiClO_4$ ion pairs with a box length of 44.32 Å.

Since the H_2O/Li ratio is not modified in this set of experiments, a similar short-range environment for the Li^+ cations is maintained in this third series of electrolytes. The linear-sweep voltammograms recorded with this series of electrolytes show 1) a gradual reduction of the electrode passivation and 2) a gradual shift of the onset potential for reduction toward less negative values when the concentration is increased. Logically, this

behavior directly results from a combination of the two extreme trends previously measured (Figure 2 and Figure 5 in the main text). Furthermore, a significant increase in the SAXS intensity at low-q with the Li-H_2O concentrations is observed, experimentally confirming the growth of these long-range $LiClO_4$-H_2O domains in this third series of electrolytes. These observations confirm the impact of the long-range organization of the water-rich nanodomains on the water reduction potential.

Supplementary References

1. Atomic form factors. http://lampx.tugraz.at/~hadley/ss1/crystaldiffraction/atomicformfactors/formfactors.php.
2. Masiker, M. C., Mayne, C. L., Boone, B. J., Orendt, A. M. & Eyring, E. M. 7Li NMR chemical shift titration and theoretical DFT calculation studies: solvent and anion effects on second-order complexation of 12-crown-4 and 1-aza-12-crown-4 with lithium cation in several aprotic solvents. *Magn Reson Chem* **48**, 94–100 (2010).
3. Åqvist, J. Ion-water interaction potentials derived from free energy perturbation simulations. *J. Phys. Chem.* **94**, 8021–8024 (1990).